



# Microstructure and morphology of Cu–Zr–Ti coatings produced by thermal spray and treated by surface mechanical attrition

Á. Révész<sup>a,\*</sup>, P. Szommer<sup>a</sup>, P.J. Szabó<sup>b</sup>, L.K. Varga<sup>c</sup>

<sup>a</sup> Department of Materials Physics, Eötvös University, P.O.B. 32, Budapest, H-1518, Hungary

<sup>b</sup> Department of Materials Science and Engineering, University of Technology and Economy, Budapest, H-1111, Hungary

<sup>c</sup> Research Institute for Solid State Physics and Optics of Hungarian Acad. of Sciences, P.O.B. 49, Budapest, H-1525, Hungary

## ARTICLE INFO

### Article history:

Received 1 July 2010

Received in revised form

10 September 2010

Accepted 27 October 2010

Available online 4 November 2010

### Keywords:

Thermal spray

Mechanical attrition

Severe plastic deformation

Cu

## ABSTRACT

Cu–Zr–Ti powders were deposited onto Cu plates by thermal spray. Upon impact onto the substrate, the particles spread out and bond well to the substrate, yielding a well adhered surface layer. The coatings then were subjected to severe plastic deformation using surface mechanical attrition treatment in a high energy SPEX 8000 shaker mill by replacing the end cap of the milling vial with the coated targets. It is demonstrated that different mechanical treatments influence the microstructural and mechanical behavior of the Cu–Zr–Ti coating, moreover, a partial solid state amorphization takes place. Roughening of the interface between target and coating ensures strong bonding while the free surface is hard and smooth. Experiments were carried out using X-ray diffraction, scanning electron microscopy, energy dispersive X-ray analysis and hardness measurements.

© 2010 Elsevier B.V. All rights reserved.

## 1. Introduction

Thermal spray is a well established procedure to synthesize coatings with a thickness of 100  $\mu\text{m}$  to enhance the surface properties, i.e. wear, corrosion and heat resistance of different engineering parts [1]. Thermal spray can be divided into several techniques based on the applied energy source to melt the starting material. In particular, flame spray (FS) consuming energy from combustion between oxygen and acetylene involves the continuous feed of a feedstock material to the tip of a spray gun where it melts in a fuel gas flame and then propelled to a substrate by the compressed gas stream [1–3]. As the molten particles impinge on the target, they cool down and build up a lamellar structure splat by splat forming the sprayed coating. A wide variety of feedstock materials, such as metal wires, ceramics and metallic and non-metallic powders are used. The as-sprayed coating is usually not homogeneous and it is typically characterized by a certain amount of porosity. The ultimate properties of the surface layer depend on the bonding nature between the coating and the target (it can be mechanical, chemical or metallurgical) and the processing parameters like temperature and pressure [2,4].

In order to eliminate the effect of porosity, it can be straightforward to apply a surface mechanical post treatment on the

as-sprayed coatings. The surface mechanical attrition treatment (SMAT) technique involves repeated multidirectional impacts by flying balls to induce surface hardening of bulk samples [5,6]. The impacts cause severe plastic deformation in the surface layer of the treated sample, leading to grain refinement and large grain boundary misorientation, dislocation blocks and microbands [7]. It is shown that the surface becomes chemically active, promoting the effectiveness of subsequent treatments such as nitriding [5].

In this investigation a powderized  $\text{Cu}_{60}\text{Zr}_{20}\text{Ti}_{20}$  metallic coating was initially flame sprayed onto a Cu plate and then mechanically treated using the SMAT technique by attaching the coated plate as a target to the end surface of the milling vial of a high energy shaker mill. Different milling conditions were carried out to explore the mechanism of the process and to investigate the morphology, microstructure and mechanical properties of the developed coatings.

## 2. Experimental

An ingot of nominal composition of  $\text{Cu}_{60}\text{Zr}_{20}\text{Ti}_{20}$  was prepared by induction melting of high purity (99.9%) Cu, Zr and Ti metals. Subsequently the feedstock material was powderized by mechanical attrition. The screened powder ( $\phi < 200 \mu\text{m}$ ) was deposited onto a roughened Cu target by the gas stream of high purity oxygen and acetylene applying a flame spray gun (Castolin type) resulting in a coating with an average thickness of 150–200  $\mu\text{m}$ . Typical temperature near the exit nozzle in this setup is well above the melting point of the individual components.

The mechanical treatment of the Cu–Zr–Ti deposits was carried out using a SPEX 8000 Mixer Mill. It is a high-energy shaker mill that swings the hardened steel cylindrical milling vial (inside diameter 38 mm and length 57 mm) in a complex three-dimensional pattern. The coated Cu target (disk) replacing the end cap of the

\* Corresponding author.

E-mail address: [reveszadam@ludens.elte.hu](mailto:reveszadam@ludens.elte.hu) (Á. Révész).

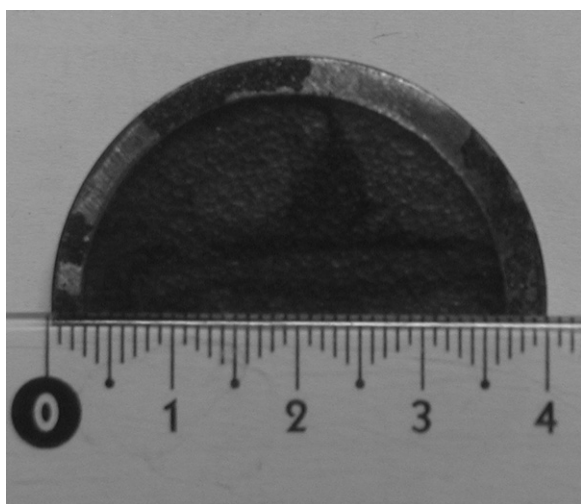


**Fig. 1.** Optical micrograph of the of the sprayed Cu–Zr–Ti coating after surface mechanical treatment for 30 min.

steel milling vial was fixed tightly to the vial. In order to ensure an approximately uniform distribution of impacts, the container was filled with a large number of hardened steel milling balls, i.e. 20 balls with a diameter of 1/4" (6.35 mm) were used for different treatment times (30 min, 90 min and 270 min). The total mass of the impacting balls was about 20 g. An optical micrograph envisages the effect of the heavy mechanical deformation occurring during the treatment (Fig. 1).

The as-deposited and mechanically treated  $\text{Cu}_{60}\text{Zr}_{20}\text{Ti}_{20}$  layers flame sprayed onto the Cu targets were used as samples for powder X-ray diffraction (XRD) measurements directly. The spectra were collected with a Philips X'pert diffractometer, using  $\text{Cu-K}\alpha$  radiation in  $\theta$ - $2\theta$  geometry, in steps of  $0.02^\circ$ . For analysis of the microstructure, surface cross sections of the treated disks were embedded in epoxy and carefully polished mechanically. The morphology was studied by a Philips XL 30 scanning electron microscope (SEM) in backscattered electron mode (BSE). Quantitative elemental analysis was carried out by energy dispersive X-ray (EDX) analysis with a relative accuracy of 1%.

Mechanical tests were carried out on the cross-section of the coatings using a CSIRO UMIS 2 device at constant load rate with an applied maximum load of 1 mN. The dynamic hardness (HV) was calculated using the Oliver–Pharr method [8].

### 3. Results and discussion

A general view of the FS deposition process can be inferred from SEM images taken on the surface and cross section of the as-sprayed coating (Fig. 2a and b). As seen, the surface contains overlapping splats with an average size of  $150\ \mu\text{m}$  accompanied with some porosity. The percentage of the porosity (15%) and the average pore size ( $40\ \mu\text{m}$ ) determined by quantitative image analyzing software (Image-J) are lower than the values obtained for flame-sprayed  $\text{Al}_2\text{O}_3/\text{TiO}_2$  coatings [9], in accordance with the lower melting temperature of the metallic components.

The complementary EDX analysis taken at several points of the coating revealed that the layer composition is  $\text{Cu}_{57}\text{Zr}_{22}\text{Ti}_{21}$ , however, some oxygen is also present in the material, which is an obvious phenomenon associated with the flame spray technique [2,10]. Experiments carried out on the cross section indicate that the as-sprayed coating exhibits a uniform thickness of  $150\text{--}200\ \mu\text{m}$ . The contrast between different layers observed in Fig. 2b indicates that individual splats can have different compositions, i.e. the darker ones are enriched in Zr ( $\text{Cu}_{46}\text{Zr}_{38}\text{Ti}_{14}$ ).

At an intermediate stage of mechanical treatment (90 min) the surface layer loses the splat-like structure and becomes more homogeneous (Fig. 3a), possessing a porosity of about 5%. Roughening of the interface between target and coating ensures strong bonding. Also note that some cracks evolve by percolation of

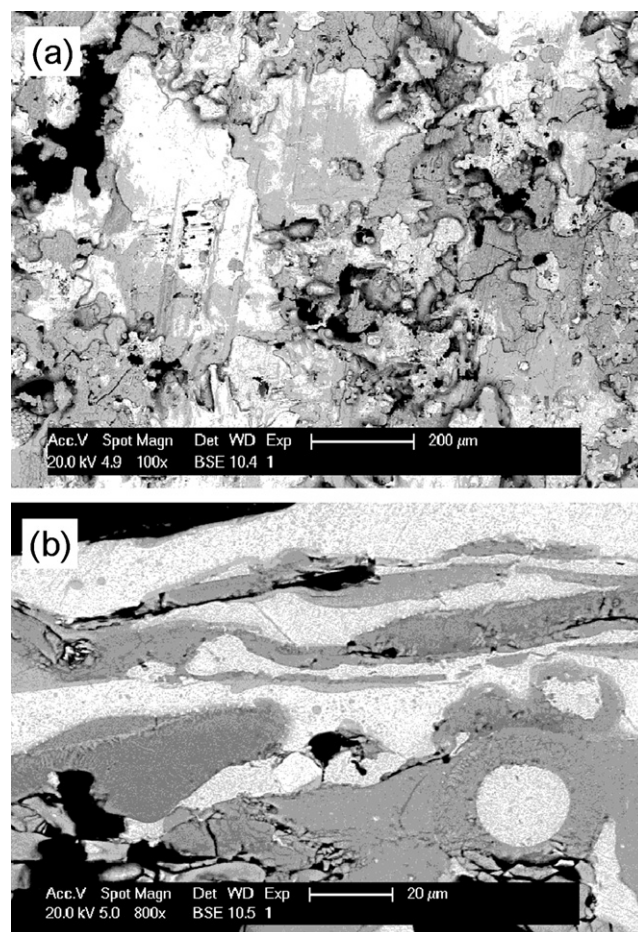


**Fig. 2.** SEM BSE images taken on the surface (a) and cross section (b) of the as-sprayed Cu–Zr–Ti coating.

the individual pores due to the severe plastic deformation. At the same time the average thickness decreases substantially to  $30\ \mu\text{m}$  accompanied with compaction, surface shearing and folding generated by the continued impacts of the milling balls [11], see the SEM BSE image of the cross section in Fig. 3b. The still continuous coating is an evidence of efficient bonding between the feedstock and the target, however, after 270 min of treatment partial break-up of the layer occurs (not shown here).

The XRD pattern corresponding to initial feedstock material reveals the formation of two equilibrium phases: hexagonal  $\text{Cu}_{51}\text{Zr}_{14}$  ( $a = 1.13\ \text{nm}$ ,  $c = 0.824\ \text{nm}$ ) and hexagonal  $\text{Cu}_2\text{ZrTi}$  ( $a = 0.514\ \text{nm}$ ,  $c = 0.823\ \text{nm}$ ) phases [12,13], see Fig. 4. Diffractograms taken from the surface of the specimens explain some aspects of the SEM images and exhibit several interesting features concerning the microstructure of the treated Cu–Zr–Ti layers. A transformation of the hexagonal phases to orthorhombic  $\text{Cu}_{10}\text{Zr}_7$  ( $a = 1.26\ \text{nm}$ ,  $b = 0.93\ \text{nm}$ ,  $c = 0.93\ \text{nm}$ ) occurs during the FS process. Apart from the oxidation of Zr, the observed sharp Bragg-peaks correspond to the Cu plate indicates that the FS deposit cannot block diffraction from the target, in accordance with the observed pores in the SEM micrograph (see Fig. 2a). As a consequence of deformation, the penetration depth of the X-ray photons becomes comparable to the thickness of the coatings developed after the mechanical treatment, therefore the corresponding patterns are dominated by the scattering from the target. Interestingly, almost no detectable peaks of the Cu–Zr(–Ti) phases are present, most

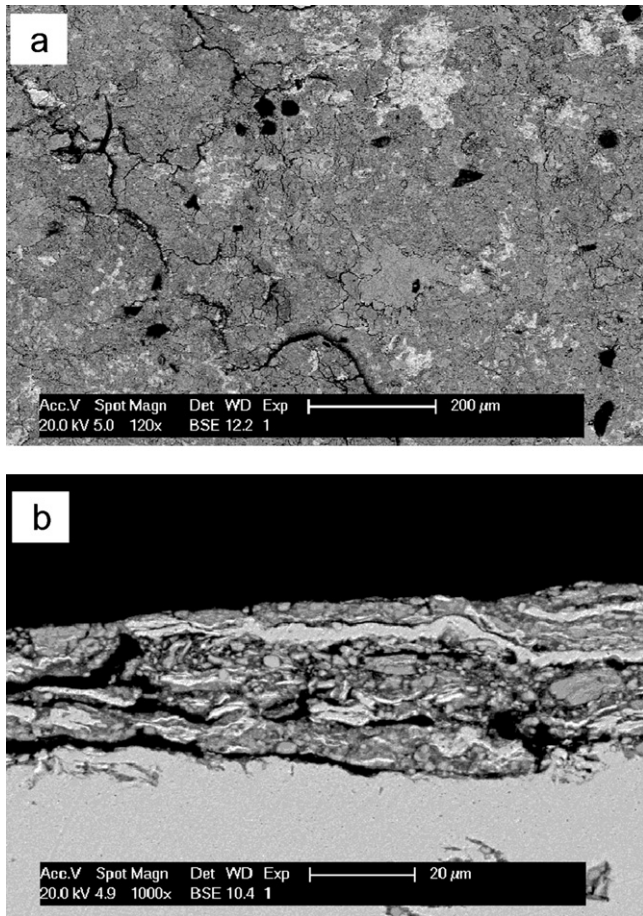


**Fig. 3.** SEM BSE images taken on the surface (a) and cross section (b) of the mechanically treated Cu–Zr–Ti coating.

probably due to significant grain size reduction and/or lattice distortions introduced by the severe plastic deformation. A clear shoulder at  $42^\circ$  after 270 min of treatment is an indicator of a possible deformation induced (partial) solid state amorphization, which is a general phenomenon of Cu–Zr–Ti ternary system [14]. By eliminating the signal corresponding to the target, the plot in the inset confirms the presence of an amorphous component.

Fig. 5 presents the hardness of the cross-section as a function of depth for the coatings. Indents separated by  $2\ \mu\text{m}$  were carried out along three parallel lines perpendicular to the coating surface. In order to reduce the effect of the rough and uneven surfaces the data were averaged for the three lines in the case of all specimens. As seen, the as-sprayed Cu–Zr–Ti layer exhibits an average HV of 2.41 GPa which is considerably higher than that of the Cu target. As the heavy deformation is introduced by the impacting balls, the surface region becomes considerably harder. After 30 min of milling the average hardness of the coating increases up to 4 GPa. The obtained thickness ( $35\text{--}40\ \mu\text{m}$ ) is in line with the SEM observations. Even though further treatment results only in partial amorphization (see Fig. 4), subsequent hardening take place ( $\text{HV} = 6.8\ \text{GPa}$ ), which is comparable that of amorphous Cu–Zr–Al [15] and Cu–Zr–Ti–Y [16] metallic glasses and exceeds the value of partially amorphized Cu–Zr–Ti by high pressure torsion [17]. The remarkably high surface hardness values can be explained by the well known Hall–Petch equation and the formation of rigid amorphous regions generated by the severe plastic deformation.

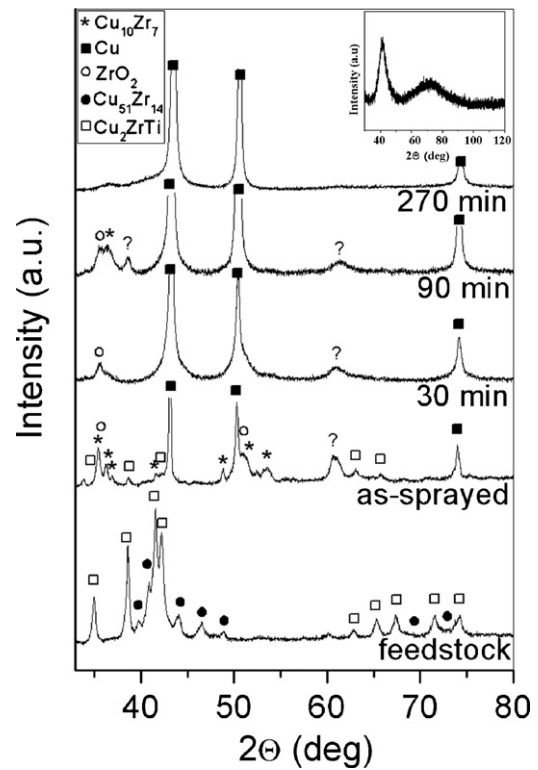


**Fig. 4.** XRD patterns corresponding to the feedstock, as-sprayed and mechanically treated disks. Inset shows the plot (270 min) by eliminating the signal of the Cu-target.

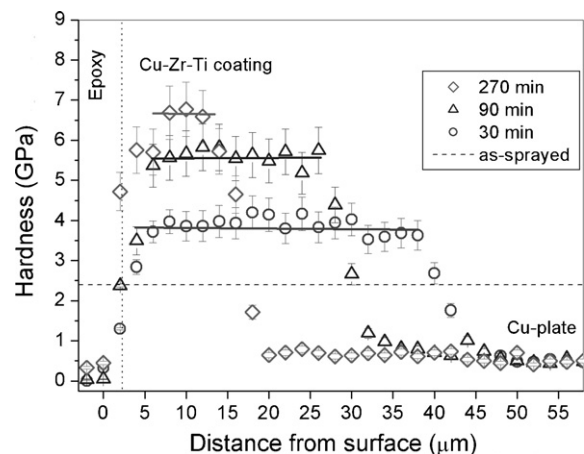


**Fig. 5.** Variation of hardness as a function of the distance from the top surface on the cross section of the coatings treated for 30 min, 90 min and 270 min. Horizontal dashed line indicates the hardness of the as-sprayed layer.

#### 4. Conclusions

Surface mechanical attrition treatment of thermal sprayed Cu–Zr–Ti coatings onto a Cu target results in microstructural and morphological changes accompanied with partial solid state amorphization due to the severe plastic deformation. At the same time the hardness of the surface layer significantly improved up to 6.8 GPa.

#### Acknowledgements

We appreciate the support of the Hungarian Scientific Research Fund (OTKA) under grant nos. 67893, 73451 and 67692. Á. Révész

and P.J. Szabó are indebted for the Bolyai Scholarship of the Hungarian Academy of Sciences. The European Union and the European Social Fund have provided financial support to the project under the grant agreement no. TÁMOP 4.2.1./B-09/1/KMR-2010-0003.

## References

- [1] M.L. Thorpe, *Adv. Mater. Proc.* 143 (1993) 50.
- [2] S. Kuroda, J. Kawakita, M. Watanabe, H. Katanoda, *Sci. Technol. Adv. Mater.* 9 (2008) 033002.
- [3] V. Katenidis, D. Chaliampalias, N. Pistofidis, G. Vourlias, E. Pavlidou, A. Stergiou, G. Stergioudis, *J. Optoelectron. Adv. Mater.* 9 (2007) 1665.
- [4] I. Ozdemir, I. Hamanaka, M. Hirose, Y. Tsunekawa, M. Okumiya, *Surf. Coat. Technol.* 200 (2005) 1155.
- [5] W.P. Tong, N.R. Tao, Z.B. Wang, J. Lu, K. Lu, *Science* 299 (2003) 686.
- [6] X. Wu, N. Tao, Y. Hong, G. Liu, B. Xu, J. Lu, K. Lu, *Acta Mater.* 53 (2005) 681.
- [7] X. Wu, N. Tao, Y. Hong, B. Xu, J. Lu, K. Lu, *Acta Mater.* 50 (2002) 2075.
- [8] W.C. Oliver, G.M. Pharr, *J. Mater. Res.* 7 (1992) 1564–1583.
- [9] K. Habib, J.J. Saura, C. Ferrer, M.S. Damra, E. Gimenez, L. Cabedo, *Surf. Coat. Technol.* 201 (2006) 1436.
- [10] S. Kumar, J. Kim, H. Kim, C. Lee, *J. Alloys Compd.* 475 (2009) L9.
- [11] Á. Révész, L. Takacs, *Surf. Coat. Technol.* 203 (2009) 3026–3031.
- [12] A. Concustell, Á. Révész, S. Suriñach, L.K. Varga, G. Heunen, M.D. Baró, *J. Mater. Res.* 19 (2004) 505–512.
- [13] Á. Révész, L.K. Varga, S. Surinach, M.D. Baró, *Mater. Sci. Eng. A* 375–377 (2004) 776–780.
- [14] Á. Révész, J.L. Lábár, S. Hóbor, A.P. Zhilyaev, Zs. Kovács, *J. Appl. Phys.* 100 (2006) 103522.
- [15] F. Jiang, D.H. Zhang, L.C. Zhang, Z.B. Zhang, L. He, J. sun, Z.F. Zhang, *Mater. Sci. Eng. A* 467 (2007) 139.
- [16] G. Zha, A. Zhang, *J. Rare Earths* 28 (2010) 243.
- [17] Zs. Kovács, S. Hóbor, P.J. Szabó, J. Lendvai, A.P. Zhilyaev, Á. Révész, *Mater. Sci. Eng. A* 449–451 (2007) 1139.